

Final Report

Generation & Global Propagation of ULF Waves

Contract No. HR0011-08-C-0009

January 31, 2010

Submitted by:

(b)(6)

BAE Systems – Technology Solutions
2000 North Fifteenth Street
Arlington, VA 22201-2627
(703) 247-4626

Distribution List:

- (a) Defense Technical Information Center
- (b) DARPA/Library
- (c) (b)(6) DARPA/CMO
- (d) (b)(6) DARPA/STO
- (e) (b)(6) DARPA/STO
- (f) (b)(6) ONR/NRL
- (g) (b)(6)
- (h) (b)(6)

Sponsored by:

Defense Advanced Research Projects Agency
Strategic Technology Office (STO)
Program: Generation & Global Propagation of ULF Waves
ARPA Order No. X126/00, Program Code: 7F40
Issued by DARPA/CMO under Contract No. HR0011-08-C-0009

The views and conclusions contained in this document are those of the authors and should not be interpreted as representing the official policies, either expressly or implied, of the Defense Advanced Research Projects Agency or the U.S. Government.

Report Documentation Page

Form Approved
OMB No. 0704-0188

Public reporting burden for the collection of information is estimated to average 1 hour per response, including the time for reviewing instructions, searching existing data sources, gathering and maintaining the data needed, and completing and reviewing the collection of information. Send comments regarding this burden estimate or any other aspect of this collection of information, including suggestions for reducing this burden, to Washington Headquarters Services, Directorate for Information Operations and Reports, 1215 Jefferson Davis Highway, Suite 1204, Arlington VA 22202-4302. Respondents should be aware that notwithstanding any other provision of law, no person shall be subject to a penalty for failing to comply with a collection of information if it does not display a currently valid OMB control number.

1. REPORT DATE 31 JAN 2010	2. REPORT TYPE	3. DATES COVERED 00-00-2010 to 00-00-2010			
4. TITLE AND SUBTITLE Generation & Global Propagation of ULF Waves		5a. CONTRACT NUMBER			
		5b. GRANT NUMBER			
		5c. PROGRAM ELEMENT NUMBER			
6. AUTHOR(S)		5d. PROJECT NUMBER			
		5e. TASK NUMBER			
		5f. WORK UNIT NUMBER			
7. PERFORMING ORGANIZATION NAME(S) AND ADDRESS(ES) BAE Systems - Technology Solutions, 2000 North Fifteenth Street, Arlington, VA, 22201-2627		8. PERFORMING ORGANIZATION REPORT NUMBER			
9. SPONSORING/MONITORING AGENCY NAME(S) AND ADDRESS(ES)		10. SPONSOR/MONITOR'S ACRONYM(S)			
		11. SPONSOR/MONITOR'S REPORT NUMBER(S)			
12. DISTRIBUTION/AVAILABILITY STATEMENT Distribution authorized to US Government agencies only; Proprietary Information; 00-00-2010; DARPA, 3701 North Fairfax, Arlington, VA, 22203.					
13. SUPPLEMENTARY NOTES					
14. ABSTRACT					
15. SUBJECT TERMS					
16. SECURITY CLASSIFICATION OF:			17. LIMITATION OF ABSTRACT	18. NUMBER OF PAGES	19a. NAME OF RESPONSIBLE PERSON
a. REPORT unclassified	b. ABSTRACT unclassified	c. THIS PAGE unclassified	7	32	

PREFACE - FINAL TECHNICAL REPORT SUMMARY

This report presents the measurement and study results of Ultra-Low-Frequency (ULF) electromagnetic waves generated by the High Frequency Active Auroral Research Program (HAARP) facility located in Gakona, Alaska. The following sections assess the performance of ULF generation by HAARP, compare ULF amplitudes at HAARP, distant monitoring sites, and from satellite, present current limited understanding of ULF propagation, discuss the fundamental science issues yet to be resolved, and recommend future efforts to improve our understanding on ULF generation and propagation by high frequency (HF) heaters.

The study documented in this report was performed by BAE Systems - Technology Solutions in Arlington, VA, under DARPA contract HR0011-08-C-0009, and directed by Dr. Chia-Lie Chang. The performance period was from January 7, 2008 to January 7, 2010.

This document was prepared at the completion of the contract and delivered to the distribution list in the cover page to fulfill the "reports and other deliverables" requirements specified in the contract.

1. Task Objectives

The High Frequency Active Auroral Research Program (HAARP) has the world most advanced ionospheric research facility. At the center of the HAARP research facility is a high power, High-Frequency (HF) phased array radio transmitter, known as the Ionosphere Research Instrument (IRI). Such instruments, also known as ionospheric heaters, are used to stimulate well defined volumes of the overhead ionosphere. In the HAARP case it is the auroral ionosphere above the IRI, which is located geographically at 62 deg 23.5 min north latitude and 145 deg 8.8 min west longitude. The IRI is complemented by an extensive suite of modern geophysical research instruments including an HF ionosonde, ELF and VLF receivers, magnetometers, riometers, a VHF diagnostic radar and optical and infrared spectrometers and cameras. These instruments, as well as instruments aboard overflying satellites, are used to observe the complex natural variations of Alaska's ionosphere as well as to detect artificial modifications produced by the IRI.

The Effective Radiated Power (ERP), bandwidth, and sweeping capability of the HAARP IRI significantly exceeds that of any other ionosphere heater, and it has been designed to produce effects not previously seen. With such capabilities, the HAARP facility opens up new opportunities for innovative technological concepts with military applications. The funded project deals with developing the technology to generate and propagate at large distances on the ground and in the magnetosphere large amounts of Ultra Low Frequency (ULF) waves in the 0.1-10 Hz frequency range. (b)(3):22 USC § 2778(e) Sec 38(e),(b)(4)

(b)(3):22 USC § 2778(e) Sec 38(e),(b)(4)

(b)(3):22 USC § 2778(e) Sec 38(e),(b)(4)

The duration of the funded Global ULF program is two years, with specific technical objectives set for each year. In the first year, the main focus is to generate ULF waves using HAARP. The technical objectives in year one are

- Demonstration of ULF generation by electrojet modulation and/or collisionless F-region heating using HF heater.
- Optimization of the efficiency of HF-to-ULF power conversion.

In the second year, the main focus is on global propagation of ULF waves artificially generated by HAARP. The technical objectives in year two are:

- Measurement of HAARP generated ULF waves at distant locations on the ground as well as from space.
- Determination of the heater operation characteristics and natural conditions that allows for optimal outreach of HAARP generated ULF waves.
- Development of theoretical and numerical models to understand the physics of ULF propagation and predict preferential propagation path.

An ultimate purpose of the funded program is to develop a quantitative understanding of the outstanding issues related to ULF generation and global propagation appropriate for transition from research to field implementation.

2. Technical Problems

2.1. ULF Generation

Generating ULF waves using ground based low frequency transmitters is practically impossible due to their large free space wavelength. The absence of having tunable, controlled, and coherent sources is the stumbling block in understanding and exploiting ULF waves for military and civilian applications. In this program, BAE Systems takes the approach of utilizing HAARP heater to create an ionospheric ULF source complemented by space and ground receivers to provide the data base needed for the development and testing of quantitative models. This program is a unique effort to explore the nonlinear behavior of the ionosphere in generating ULF waves, which has never been attempted before.

(b)(3):22 USC § 2778(e) Sec 38(e),(b)(4)

(b)(3):22 USC § 2778(e) Sec 38(e),(b)(4)

The concept of using ground based HF heater to modify ionosphere for the purpose of generating low frequency electromagnetic waves has been put into practice for several decades. The most successful example has been the generation of ELF/VLF waves using the HF heaters. The technique of ELF/VLF generation relies in modulation of ionospheric electrojet currents with HF waves radiated from the ground transmitters. Specifically, powerful HF waves can very efficiently heat the electrons in the ionospheric D/E layer. The resultant periodic modification of the electron temperature leads to modification of the plasma conductivity due to the temperature dependence of the electron neutral collision frequency. Subsequently, the changes in plasma conductivities lead to modification of the ambient electrojet current system. If the transmitter is switched in an on-off cycle at a particular frequency, the electrojet current will also be periodically modulated. As a result the heated ionospheric volume with its surrounding region operates as a large antenna radiating at a frequency corresponding to the frequency of the on-off heating cycle. The resultant ELF/VLF waves are subsequently injected downwards in the earth-ionosphere waveguide propagating laterally as TE and TM modes and upwards in the ionosphere propagating towards the conjugates as whistler modes. There are many experimental and theoretical papers addressing the technique.

The approach to generate ELF/VLF waves using the ground based HF heater has been extended to generate ULF waves in the funded program. ***The most critical technical problem is to identify the ULF generation mechanisms.*** We have tried two different ULF generation mechanisms, and both have led to very successful outcome. The first relies on traditional electrojet modulation of the D-region of the ionosphere. The second relies in modulated collisionless heating of the F-region and does not require an electrojet. The second mechanism is more appealing because it does not rely on the occurrence of electrojet, which is not frequent at the location of HAARP.

2.2. ULF Propagation

The ULF waves generated by HAARP can propagate in two separate directions. In the upward direction, the ULF waves can propagate into the magnetosphere following the Earth's magnetic field. In the lateral direction, ULF waves can propagate either in the ionospheric duct at the F layer, or in the earth-ionospheric waveguide between the ground and the bottom of the ionosphere. It is mainly the lateral propagation that is of interest to the funded program because it provides global coverage in the ULF band of frequencies.

The global propagation of ULF waves, especially in the so-called Pc1 range (0.1-10 Hz), has been studied extensively by space science community using naturally occurred Pc1 micropulsations as the source. The short-period pulsations in the Pc1 band are generally associated with plasma processes near or above the ion gyro-frequencies, which are generated locally in the plasma at the equatorial magnetosphere by ion cyclotron instabilities. Observations of Pc1 pulsations at global locations indicate that they travel along the earth's surface over thousand kilometer distances in the ionospheric MHD waveguide, illustrated by Figure 1. It was the global occurrence of Pc1 that gave the first indirect clue to the idea of horizontal propagation of Pc1 in the ionospheric layers in the form of magnetosonic waves. A key observation gave further credence to concept of the ionospheric waveguide. Namely, it was noted that ULF pulsations with frequencies higher than 0.2-0.5 Hz were observed simultaneously at widely spaced locations. The presence of a lower frequency in the spatial distribution of Pc1 was a good indirect indication that the pulsations propagate in horizontally in a waveguide with cut-off frequency of 0.2-0.5 Hz. Direct measurements found that the horizontal propagation velocity of Pc1 was approximately 500-700 km/sec. This velocity corresponds to the velocity of magnetosonic waves in the F-region of the ionosphere.

The physics underlying the propagation can be understood, in terms of geometric ray theory for magnetosonic waves. As is well known a ray in a stratified isotropic medium bends towards increasing refractive index $\eta(z)$, or in other words, the ray is convex in the direction of decreasing $\eta(z)$, where z is the vertical direction. As a result wave propagation in the horizontal direction is possible if the refractive index $\eta(z)$ has maximum. The ionosphere can be approximated as an horizontally stratified plasma and the magnetosonic waves are almost isotropic with $\eta = c/V_A \propto n^{1/2}$, where $n(z)$ is the plasma density. Since $n(z)$ has a maximum at the F-region at an altitude of 250-300 km, it can be expected that under some conditions the rays of the magnetosonic waves are trapped in the ionospheric layers (see Figure 1).

While this consideration demonstrates the possibility of ducting magnetosonic waves along ionospheric layers, it ignores several important features of the Pc1 waves. These include penetration into the ground, mutual transformation between magnetosonic and shear Alfvén waves and the role of anisotropy. It appears that in general Joule dissipation in the D region dominates over mode conversion when the Pedersen

conductivity of the lower ionosphere exceeds the Hall conductivity. If the Hall conductivity dominates then mode conversion becomes important resulting in quasi-periodic wave attenuation. Theory and observations indicate that the waveguide attenuation varies from 1 to 10 dB/Mm, and that daytime attenuation is significantly higher than nighttime. Finally, a major discrepancy between theory and experiment is the fact that Pc1 appear to propagate predominantly in the equatorial direction rather than towards the poles despite the fact that the horizontal projection of the Alfvén rays incident on the ionosphere has a poleward component

Even though physical understanding of the nature of ULF pulsations has been greatly improved in the last three decades due to major advances in experimental techniques and theoretical work, understanding the propagation characteristics is still in its infancy due to lack of a well characterized localized ULF source. Therefore, *the critical technical problem is to develop physical understanding of ULF propagation characteristics*, including the propagation path, the attenuation, and the dependence on environmental conditions. With HAARP being developed as a reliable source for ULF waves in this program, we are able to perform near field and far field measurements at various locations to validate propagation models and to optimize ULF power injection to the desired propagation paths.

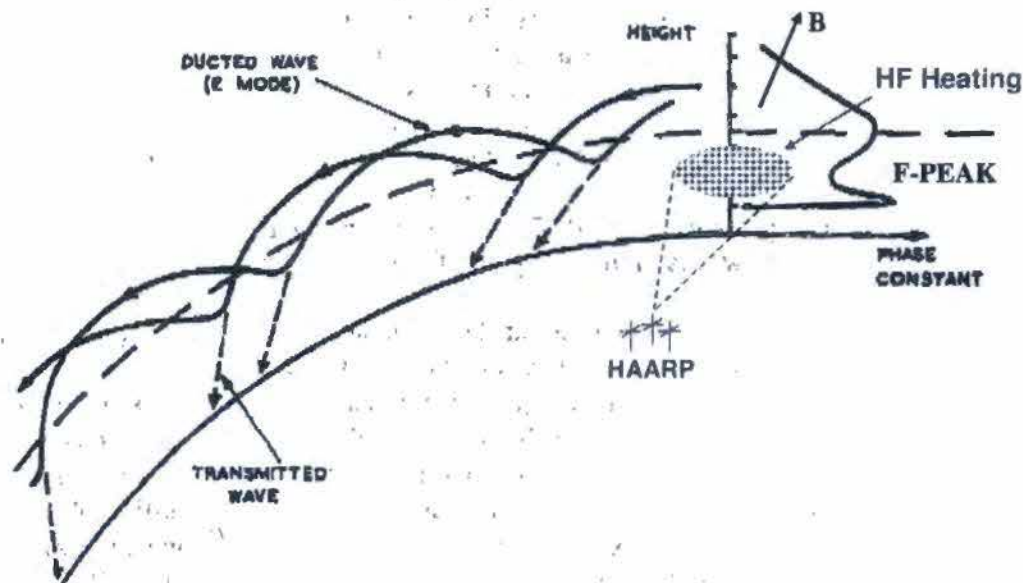


Figure 1. Generation and injection of magnetosonic waves by F-region, collisionless heating at the upper hybrid frequency. HAARP induced F-region heating modulated at ULF frequencies results in periodic modulation of the F-region plasma pressure and generation of isotropic magnetosonic waves. The waves, whose ray paths are shown in the figure, are trapped in the Alfvénic duct reflecting downwards due to the gradient in the Alfvén velocity above the F-region plasma density peak. Ground penetration occurs either by tunneling through the D-region or by generation of a Hall current by the horizontal electric field of the magnetosonic mode.

3. General Methodology

3.1. ULF Generation

As mentioned in the previous section, there are two different ULF generation mechanisms. The first relies on traditional electrojet modulation of the D-region of the ionosphere, while the second relies in modulated collisionless heating of the F-region and does not require an electrojet. The latter option removes the restriction for locating HAARP type facilities in electrojet regions.

3.1.1. Modulation Waveform

The fundamental technique for ULF generation is to modulate ionosphere with periodic heating pulses with the use of HF transmitters on the ground. Depending on the carrier frequency of the HF waves and the ionospheric profile, periodic heating and cooling cycles can cause modulations of plasma properties at different heights of ionosphere.

(b)(3);22 USC § 2778(e) Sec 38(e),(b)(4)

(b)(3);22 USC § 2778(e) Sec 38(e),(b)(4)

(b)(3);22 USC § 2778(e) Sec 38(e),(b)(4)

(b)(3);22 USC § 2778(e) Sec 38(e),(b)(4)

However, actual mechanisms of EM emissions depend on the altitude of the modulated region.

3.1.2. Electrojet Modulation (D/E Region)

When the HF carrier frequency matches plasma frequencies in the D (< 75 km) or lower E (80-120 km) regions, the heater wave is strongly absorbed in these regions. Periodic electron heating in the Hall (lower E) dominated region in the lower ionosphere modulates the conductivity of the heated spot. In the presence of electrojet current in this region, as electron flow is affected by the changing conductivities, polarization charges start to build up at the lateral boundaries of the heated spot. Such charge build-up launches a pair of current carrying whistlers at the modulation frequency. The downward whistler driven current closes in the Pederson dominated region and creates currents that couple to the Earth-Ionosphere (EI) waveguide. These oscillatory currents will radiate EM waves like giant antenna in space, at the specified modulation frequencies of the heater pulses. For modulation frequencies above the Schumann resonance (≈ 8 Hz) the waves have been observed to propagate at large lateral distances. For modulation frequencies below 8 Hz the modes can only be detected in the vicinity of the heated spot since they are evanescent and their power decays as $1/R^4$. The upward propagating whistlers are guided by the magnetic field lines or any available ducts to the conjugates. VLF waves have often been detected by over flying satellites and measurements at the HAARP conjugate regions by receivers placed on buoys and on passing ships. For modulation frequencies below the Oxygen gyro-frequency (≈ 25 Hz) we expect that the current front propagating upwards will be mode converted at an altitude of 120 km, where the oxygen ions become magnetized, and propagate towards the conjugates as guided Shear Alfvén (SA) waves.

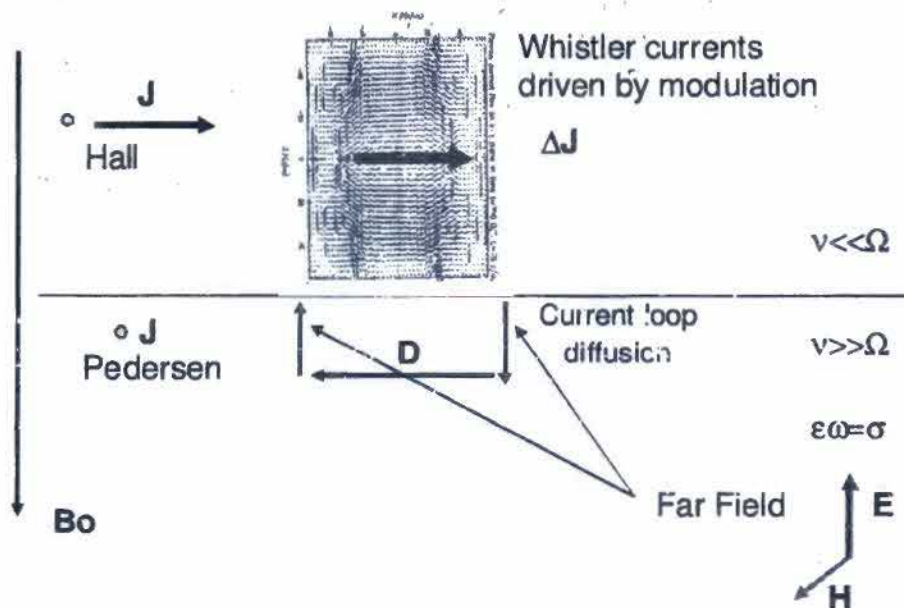


Figure 3. Vertical current loop in the ionosphere from HF modulation in D/E regions. Red arrow indicates modulation of Hall current. Such current loops radiate electromagnetic waves at the modulation frequency of the HF pulses.

3.1.3. Ionospheric Current Drive (F Region)

When HF frequency matches closely to critical plasma frequency (f_oF2) at F layer, and "O" mode polarization is selected for the HF beam, electron heating occurs near the F peak (250-300 km altitude). Modulation of the electron temperature in the F region results in modulation of plasma pressure. The oscillating pressure gradient $\nabla \delta p$ in the heated volume generates a diamagnetic current \mathbf{J} given by

$$\bar{\mathbf{j}} = \frac{\bar{\mathbf{B}} \times \nabla \delta p}{B^2} \exp(i\omega t) \quad (1)$$

Here B is the ambient magnetic field, δp the variation of the plasma pressure and ω the modulation of the HF power. Note that the F-region heating and cooling rates are sufficiently fast to allow for modulation at ULF but not at ELF or VLF timescales.

If the shape of the heated region is disk like, as shown in Figure 4, a circular current loop will be induced at the edge of the disk due to pressure gradient. Since the induced current loop is horizontal, its radiating moment is vertically aligned with the ambient magnetic field, and the resulting radiation fields are predominantly magnetosonic waves with magnetic vectors parallel to the ambient magnetic field. Propagation direction of magnetosonic waves is isotropic in homogeneous plasma. However, due to density increase in the F layer, magnetosonic waves may be guided along a horizontal duct formed by density increase in the F layer. The MS waves have been detected by satellites over much larger regions than the HAARP site field line and in the presence of the MS duct will be detected at significant lateral distances.

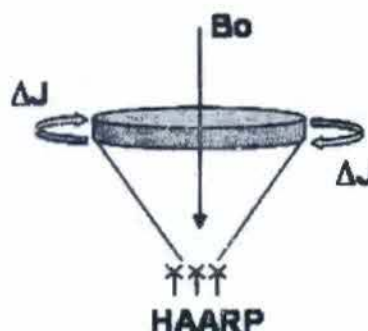


Figure 4. Circular current loop is generated by F layer modulation

3.2. ULF Propagation

ULF waves are confined and guided by a number of geometric structures surrounding the Earth. These structures play a critical role in the excitation and transmission of ULF signals from the source to the receiving sites. There are the well known Earth-Ionosphere waveguide and Shumann resonator, the magnetosonic duct surrounding the F-region of the ionosphere, two ionospheric resonators (LAR) between the D/E region of the ionosphere and few thousand kilometer altitude along the magnetic field line surrounding the source, the magnetospheric duct between two conjugate hemispheres and large magnetospheric resonators for Alfvén (Field-Line Resonances) and compressional waves. All of the above exert strong influence on the natural background and sporadic emissions.

The study of ULF propagation characteristics relies on several observational approaches. The first approach is to measure ULF waves at multiple locations on the ground. The second approach is to measure ULF waves from space. And the final approach is to understand ULF propagation properties using numerical models. All three approaches were used in this program.

3.2.1. Ground Measurements

3.2.1.1. ULF Measurement Sites

During the program period, HAARP experiments were performed to generate ULF signals in the 0.1 Hz – 20 Hz frequency range by ionospheric modulation. Magnetic signals were detected on the ground by induction magnetometers of high sensitivity deployed at various locations. (b)(3):22 USC § 2778(e) Sec 38(e),(b)(4)

(b)(3):22 USC § 2778(e) Sec 38(e),(b)(4) The temporary sites operate on campaign basis. Table 1 and Figure 5 show the geographical location of these sites and their relative distance to HAARP.

Permanent Sites	Distance to HAARP (miles)
Gakona, Alaska	8
(b)(3):22 USC § 2778(e) Sec 38(e),(b)(4)	
Temporary Sites	Distance to HAARP (miles)
Homer, Alaska	220
Kodiak, Alaska	377
Juneau, Alaska	482

Table 1. Location and distance of ground measurement sites to record HAARP-ULF waves.

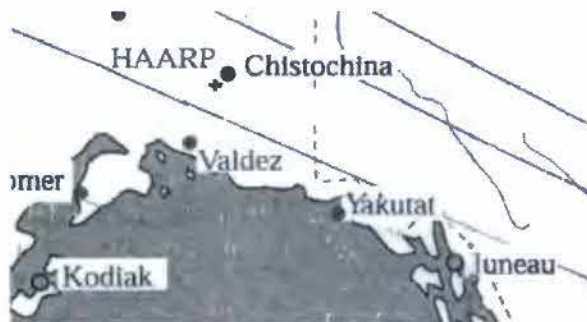
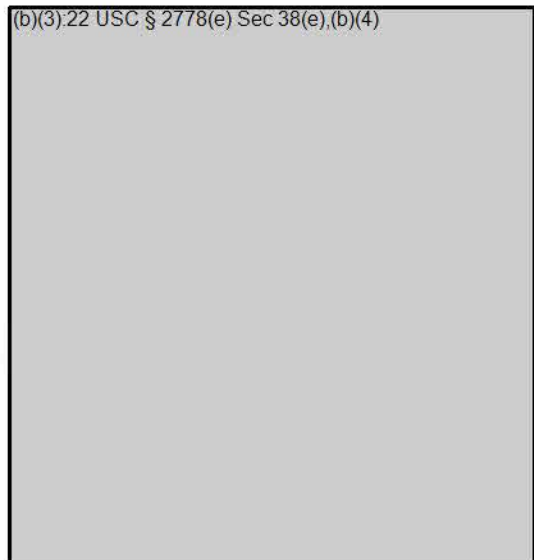


Figure 5a. Temporary ULF sites at Homer, Kodiak, and Juneau Alaska.



3.2.1.2. Magnetic Measurement of ULF Waves

The instrument used in the program to detect ULF waves at measurement sites is induction magnetometer, which measures magnetic components in the ULF fields. (b) (3) (2)

(b)(3):22 USC § 2778(e) Sec 38(e),(b)(4)

(b)(3):22 USC § 2778(e) Sec 38(e),(b)(4) Magnetic fields at each site were measured in 2 dimensions, by two induction magnetometers aligned with magnetic north-south and east-west directions, respectively. The vertical component of the magnetic field was not measured because its amplitude was an order of magnitude less than its horizontal counterparts. (b)(3):22 USC § 2778(e) Sec 38(e),(b)(4)

(b)(3):22 USC § 2778(e) Sec 38(e),(b)(4)

(b)(3):22 USC § 2778(e) Sec 38(e),(b)(4)

3.2.1.3. Data Processing

Data analysis was performed in two phases: initial data analysis (quick look) at the end of each day's experiment, and detailed analysis performed after the completion of data acquisition. The initial analysis examined the spectral content computed from the time series magnetic data collected after each day of ULF experiment. Specifically, "quick-look" spectrogram images were produced for the time varying magnetic fields and visual identification of artificial ULF signals and peaks of Schumann resonances were performed to route out any errors in the data collection and processing. When the initial data analysis indicated that a usable signal was present and the data were gathered and processed correctly, more detailed analysis was performed. The detailed analysis consisted of isolating the ULF signals in the spectrogram and extracting its amplitude and phase out of magnetic time series data. The ultimate goal of data analysis is to produce a tabulated ULF signals detected on the ground according to HAARP operational characteristics, such as HF frequency, polarization, heater waveform, and local ionospheric conditions including the existence of electrojet currents, D/E/F layers, and critical foF2 frequency.

3.2.2. Satellite Observations

Artificial ULF waves generated by HAARP can also be detected by the satellites in space. Such detection was made in the program by analyzing the particle and electric field data collected by the DEMETER satellite when it flew over the HF heated spot. The DEMETER satellite is a French satellite that is designed to monitor EM signals emitted prior and during the earthquake. It moves around the earth in a low earth orbit (LEO) with an altitude approximately 650 km above ground and an inclination of 86° . Figure 8 shows the photo of the DEMETER satellite and its ground tracks.

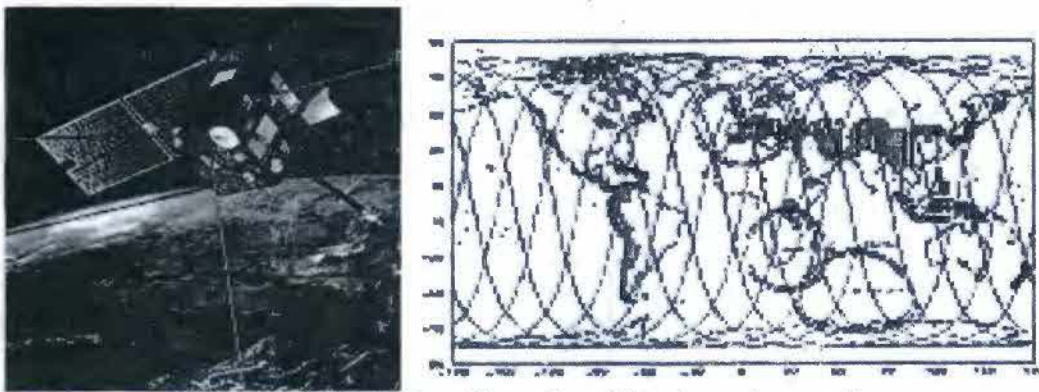


Figure 8. DEMETER satellite and its orbit tracks on the ground.

Instrument onboard DEMETER measured the ULF waves generated by the F-region modulation. The satellite detection provides us with a unique opportunity to estimate the overall radiated power and the HF to ULF conversion efficiency. In planning the ULF measurements we focused on satellite passes close to the magnetic zenith of HAARP, defined at the satellite altitude at the center of the magnetic force tube intersecting the heated region in the ionosphere. While the scientific objectives of the DEMETER satellite were to study ionospheric disturbances caused by seismo-electromagnetic effects

[Parrot et al. 2006], its instrumentation and orbit is ideal for measuring ionospheric disturbances driven by CW and modulated ionospheric HF heating. The data analyzed in the program comes from the electrical field instrument (ICE) and the plasma analyzer which measures the ion density and temperature.

3.2.3. Modeling of ULF Propagation

Computational models were built in the program to simulate horizontal propagation of ULF compressional Alfvén waves produced by a localized source such as HAARP. The first model was a two dimensional Alfvén wave propagation model. The theoretical formulation and the numerical framework was developed and published by Lysak [Lysak, 1997]. This model uses a constant vertical magnetic field, and can use any arbitrary stratification of the ionospheric plasma density and the Hall and Pedersen conductivities. The 2D simulation region extends from 70km-8000km with a grid spacing in the vertical (z-) direction that varies from 5km-250km in such a way as to always satisfy the Courant condition. In the horizontal (x-) direction it covers 5000km with a constant horizontal spacing of ~40km. In later part of the program, this 2D model was upgraded into a 3D model to study the effect on propagation of sweeping the heater beam that breaks the symmetry of the problem. This 3D model includes an additional (y-) direction with a constant grid spacing of ~40km. The 3D model explicitly advances the compressional and shear Alfvén waves and can use a current drive [see Lysak, 1997], but for our simulations we drove the compressional wave directly at the height where the plasma density is maximum, ~370km. By changing the plasma density we created ionospheric profiles with different F_oF₂ frequencies. We kept the conductivity profiles constant throughout our simulations, with a Hall region extending from 70km-130km.

4. Technical Results

Technical objectives in this two-year program are structured on yearly basis. The objective for year one is the characterization of ULF generation by HAARP-IRI. This objective is achieved through demonstration of ULF generation by:

- Modulating auroral electrojet currents;
- Modulating F layer of the ionosphere in the absence of electrojet activities.

The validation of ULF generation is based on near-site measurements by induction magnetometers located at Gakona, Alaska. The objective for year two is the study of global propagation properties of HAARP generated ULF waves. This objective is achieved by analyzing:

- Data collected at multiple ground ULF receiving sites;
- Data taken by overflying DEMETER satellite;
- Results from computational models.

In this section, highlights of technical results from generation and propagation studies are presented.

4.1. HAARP ULF Campaigns

A series of ULF campaigns were conducted in a period from April 2008 to October 2009. These campaigns took place after the upgrade project of the HAARP-IRI facility was completed. Therefore, these campaigns took full advantage of a HF heating facility that is capable of delivering its peak power at 3.6 MW level. In Table 2, ULF campaigns occurred in this program period (April 2008 to October 2009) and two of the earlier ULF campaigns at HAARP (April and September 2007) are listed. For reference purpose, each campaign is numbered sequentially according to its date of occurrence.

No.	ULF Campaign	Distant Sites	ULF Events	ELF Events	Frequencies Hz
1	April 2007	Juneau	2		(1)
2	September 2007	Kodiak		6	(15, 20)
3	April 2008	(b)(3):22 USC § 2778(e) Sec 38(e),(b)(4)			
4	August 2008 (Day)				
5	September 2008				
6	December 2008				
7	May 2009				
8	August 2009 (Day)				
9	September 2009				
10	October 2009-ULF				

Table 2. List of HAARP-ULF campaigns held prior to the program (1,2) (b)(3):22 USC § 2778(e) Sec 38(e). Column 2 is campaign month. Column 3 is distant sites (other than Gakona, AK) with ULF measurements. (b)(3):22 USC § 2778(e) Sec 38(e),(b)(4) Column 5 is number of Low ELF (10-50Hz) events detected. Column 6 is frequencies associated the observed ULF/Low ELF events.

4.2. ULF Generation Mechanisms

As mentioned in Section 3.1, there are two physical mechanisms for ULF generation: electrojet modulation in the polar region (PEJ) and ionospheric current drive in the F region of the ionosphere (ICD). We can draw distinction between these two cases by analyzing the data at Gakona, AK, which is directly under the heated area. Specifically, we compare the amplitude of the 1 kHz marker operation with the amplitude of the ULF waves. In the presence of electrojet, which is an infrequent event at HAARP, the marker modulation excites measurable 1 kHz signals on the ground, with amplitude of the 1 kHz directly proportional to the strength of the electrojet. Therefore, the 1 kHz marker is a good benchmark of the electrojet strength. When electrojet is strong, modulation at ULF frequencies will yield similar amplitudes to modulation at 1 kHz. By contrasting ULF and 1 kHz amplitudes in the same modulation waveform shown in Figure 2, we can say that electrojet modulation is the modus operandi if i) the 1 kHz amplitude is large (> 1 pT); and ii) the ULF amplitude is comparable to 1 kHz amplitude. Examples of electrojet modulation is provided in the following sub-section.

4.2.1. Electrojet Modulation (D/E Region)

Figure 9 shows the plot of the ULF signal amplitude against the 1 kHz marker amplitude that is used as a proxy for the electrojet strength, from data collected in Campaigns #3. The dashed lines in these plots indicate that ULF and marker amplitudes are equal. As we can see from Figure 9, most data points distribute along and around dashed line, indicating that ULF and marker amplitudes are comparable in magnitude. Therefore, we can deduce that electrojet modulation is the dominant physical mechanism for ULF generation in Campaign #3.

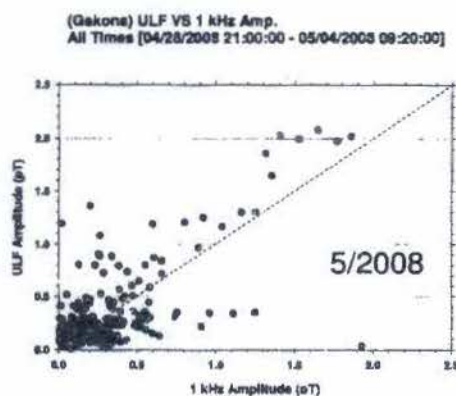


Figure 9. ULF vs. 1 kHz marker amplitude recorded at Gakona, AK in Campaign #3.

4.2.2. Ionospheric Current Drive (F Region)

Figure 10a & 10b show the plots of ULF amplitude vs. 1 kHz amplitude for Campaigns #9 & #10, respectively. From these plots, we can see that data points lie way above dashed lines, indicating that ULF amplitude exceeds marker amplitude by a big margin. This is in contrast to the electrojet modulation case shown in the last section. In these campaigns the HF modulation technique generated preferentially ULF waves rather than kHz waves. Therefore, the physical mechanism of ULF generation is very different from electrojet modulation. The other important clue is the ULF and 1 kHz amplitudes in these plots. The maximum amplitude is at 1 pT or less. While it is very common to generate 1 kHz exceeding 1 pT during an electrojet, such low amplitude of kHz generation suggests that it is not electrojet modulation in these campaigns.

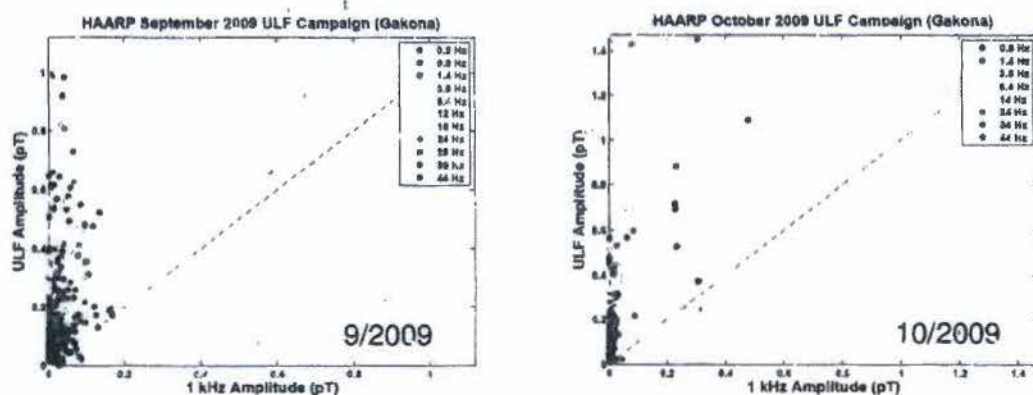


Figure 10. ULF amplitude vs. 1 kHz amplitude measured at Gakona, AK from left: (a) September 2009 campaign (#9), and right: (b) October 2009 campaign (#10).

In the cases shown in Figure 10, the ULF generation was achieved by modulating F layer of the ionosphere with HF pulses. Schematic of the physical mechanism is presented in

Figure 4. In addition to ULF waves (0.1 to 10 Hz), waves in the low ELF frequency range (10 – 50 Hz) were also generated without the presence of electrojet current. We will have more discussions on these issues in later part of the report.

4.2.3. Technique to Achieve ICD

The results of ULF generation in the absence of electrojet are very interesting because it eliminates the need to wait for the infrequent occurrence of auroral electrojet, thus removing a stumbling block for developing a practical system. The key question is how to prove that these ULF waves were generated by modulating the F layer. Systematic survey of modulation parameters was performed in Campaigns #9 and #10. In the September campaign (#9), ULF modulation was performed from twilight to past midnight hours (6PM – 4 AM) in local Alaska daylight saving time. During this 10-hour period of experiment, ionosphere declined with time as solar luminance faded out gradually. Figures 11a and 11b show the change in ionosphere property in local ionograms taken by onsite ionosonde at HAARP.

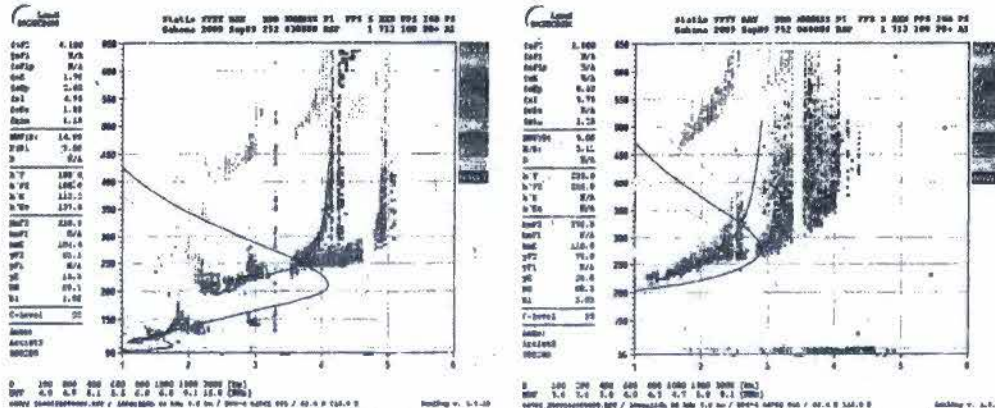


Figure 11. Local ionograms at HAARP site on September 8, 2009, at left: (a) 6PM ADT, and at right (b) 9PM ADT. The lower E layer at altitude 100-180 km in (a) disappear completely in (b).

From Figures 11, it is clear that the so called E layer of the ionosphere (from 90 km to 180 km) existed at 6PM disappeared completely from 6Pat 9PM. This is because sunlight supporting and sustaining plasma in the E region is faded away starting at nautical twilight, thus the plasma population. By 9PM, plasma in the E region is completely gone due to recombination. Therefore, the F layer is exposed for HAARP modulation after 9PM at even the lowest available HF frequency, which is 2.75 MHz. In other words, any HF modulation done 2 hours after nautical twilight in September Campaign (#9) is directly on the F layer of the ionosphere. The most effective way to perform F layer modulation, and to induce current drive in that region, is to conduct pulsed heating after the lower (D/E) layers disappear. However, the F layer is also declining after sunset and at some point in time there will be no F layer to modulate with. Thus there is a time window for F layer modulation, and for ionospheric current drive at F.

This important point can be made more clearly by Figure 12. In this figure, ionospheric parameters indicative of plasma density in the E and F layers are plotted as functions of time. The so-called foE and foF2 are the peak plasma frequencies of the E and F2 layers, respectively. The HF frequencies used to modulate ionosphere on 2009-09-09 UTC and 2009-09-10 UTC are plotted as red crosses. From Figure 12, we can see that the E layer (foE) went away at around 05:00 UTC (8PM) at both days. The peak F indicator, foF2, declined with time and went away at around 12:00 UTC (3AM) at both days. Therefore, the F layer modulation was achieved most effectively from 05:00 to 12:00 UTC (8PM to 3AM), without losing any of the HF energy to the lower (D/E) layers. To summarize, the optimal way to deliver maximum power to the F layer and to accomplish ionospheric current drive is in the time period from no foE to no foF2.

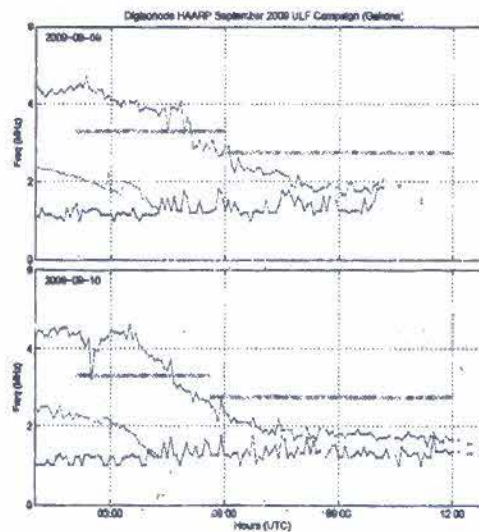


Figure 12. Strength of E & F regions (foE & foF2) are plotted vs. time for 09-09-2009 and 09-10-2009 UTC.

4.2.4. ULF to Low ELF Generation by ICD

Electromagnetic waves in the ULF (0.1-10 Hz) and low ELF (10-50 Hz) can be generated by current drive, or equivalently F layer modulation at these frequencies. Figure 13 shows the magnetic field amplitude measured at Gakona during the dates and time periods in Figure 12. The wave amplitudes are separated into three frequency groups in this figure. The 1 kHz marker is shown as a thin black line. The ULF waves are shown in thick color thick bars, and the low ELF waves are shown in thin color bars. From the 2009-09-09 plot, we can see that the 1 kHz amplitude is only significant when the foE is non-zero, or equivalently when E layer is present. Both ULF and low ELF amplitudes start to grow after E layer disappears, or foE becomes zero. Their amplitudes reach about 0.3 pT at 11:00 UTC. The 2009-09-10 plot exhibits a similar pattern. That is, when E layer is

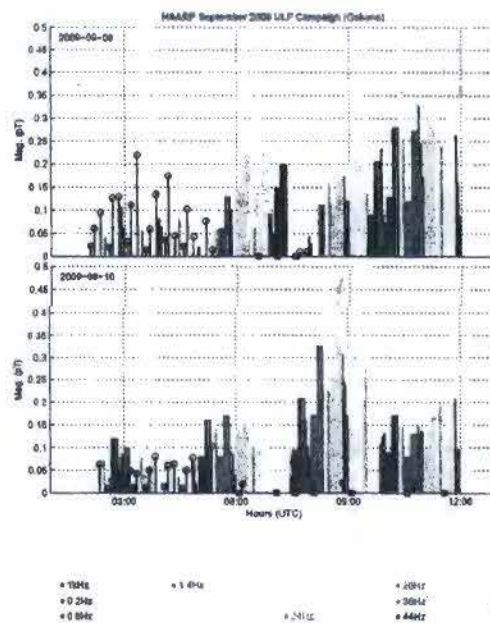


Figure 13. Amplitudes of kHz, ULF, and low ELF waves at Gakona, AK are plotted vs. date and time as shown in Figure 12.

present before 05:00 UTC, all amplitudes

(including 1 kHz marker) are small. However, after E layer disappear at about 05:00 UTC, both ULF and low ELF amplitudes start to increase, while the 1 kHz amplitude starts to decrease. The ULF and low ELF amplitudes reach peak of 0.4 pT about 09:00 UTC and decline afterward. The decline is probably due to decreasing F layer plasma density (or decreasing foF2) as shown in Figure 12.

An important feature in Figure 13 is the amplitudes of two low ELF frequency stepping, (12, 18, 24 Hz) and (28, 36, 44 Hz) triplets, after the ULF bars. Figure 14 shows a blow up picture of these triplets in 2009-09-09 from 10:00 to 12:00 UTC. From this figure, we can see that the amplitudes in these triplets decrease with increasing frequency. For instance, the last triplet 28, 36, 44 Hz on the right most part of the plot, amplitudes are 0.22, 0.14, and 0.08 pT, respectively. The decrease of amplitude with increasing frequency of modulation is a typical feature of F region modulation. This is because both the heating time and the relaxation time are long compared with the lower layers (D/E). Therefore, modulation response of the F region decreases as modulation period becomes shorter, or modulation frequency becomes higher. Base on extrapolation, the maximum modulation frequency F region will respond to is about 50 Hz, which extends from

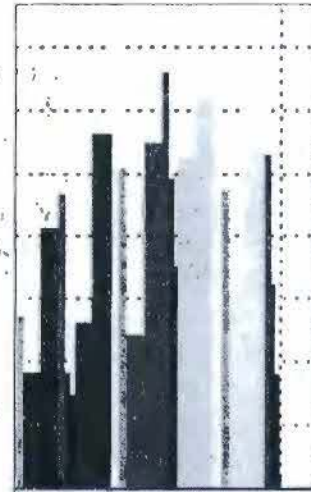


Figure 13. Expanded plot of low ELF triplets for 2009-09-09 from 10:00 to 12:00 UTC

ULF to low ELF frequency bands. To summarize, the most effective range of frequency for ionospheric current drive (ICD) in the F region is from 0 to 50 Hz.

The advantage of ICD versus electrojet modulation is that ICD can be done predictably and consistently on daily basis. To illustrate this point, Figure 14 shows ULF/ELF amplitudes measured in 9 consecutive days in the October 2009 campaign, from October 14 to 22. In this figure, the ELF amplitudes from 12 to 44 Hz are plotted in thick colored bars. The VLF amplitudes from 100 Hz and above are plotted in thin vertical lines. It can be seen that low ELF generation in the 10-50 Hz band is consistent from 10-14 to 10-21, with amplitude from 0.1 pT to 0.4 pT on daily basis. The only exception is on Oct. 22, when the VLF amplitudes are significantly larger than the ELF amplitudes throughout the day. Note that

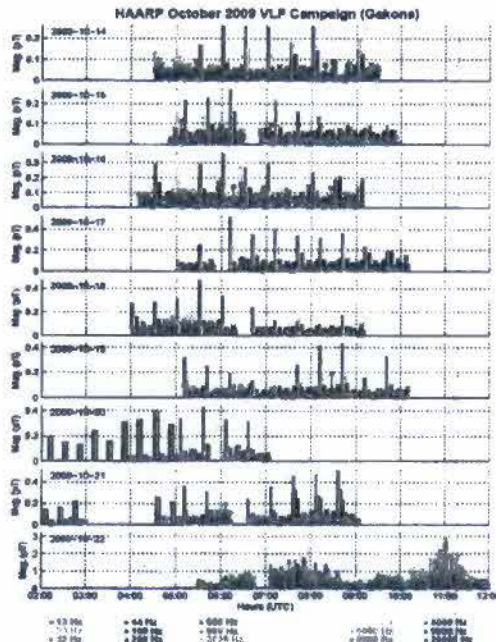


Figure 14. ELF generated by ICD from 10-14 to 10-21 in October 2009 campaign. ELF generated by electrojet modulation is on 10-22 only.

the amplitude scale on this day is significantly higher than the previous days. What makes this day so unique is the onset of strong electrojet current above HAARP. Therefore, the measured amplitudes are due to electrojet modulation, which is in sharp contrast with F region ICD dominated in previous days.

4.2.5. ULF Generation Efficiency - ICD vs. PEJ

It is instructive to show the results of modulation amplitude based on two very different physical mechanisms, namely the ionospheric current drive (ICD) versus the polar electrojet (PEJ) modulation. Figure 15 shows the generation efficiency that is defined as the normalized amplitude over a broad frequency spectrum, ranging from 10 Hz at the low end to 20 kHz at the high end. The amplitude normalization is taken to be the ratio of amplitude at a particular frequency to that at the 2 kHz modulation in adjacent time. By normalizing to 2 kHz, we can isolate amplitude variation due to temporal variation of the electrojet strength. The generation efficiency of ICD is shown in Figure 15a. In this figure, we can see that the efficiency increases with decreasing frequency below 50 Hz as described in Sec. 4.2.4. The efficiency above 50 Hz is low and remains constant all the way up to 20 kHz. The generation efficiency of electrojet modulation (PEJ) is shown in Figure 15b. In this figure, we can see that the efficiency is peaked in the 2 kHz to 10 kHz range. The efficiency decreases with increasing frequency above 10 kHz. This is because the limit of the heating and cooling times at lower ionosphere (D/E) layers are about 0.1 msec. Efficiency declines when modulation period is shorter than this time limit. For frequency below 10 Hz, we can also see a gradual increase in efficiency with decreasing modulation frequency. However, the overall level at less than 10 Hz is a factor of 3 smaller than the level at 2 kHz. This trend is just the opposite to that of the ICD case in Figure 15a.

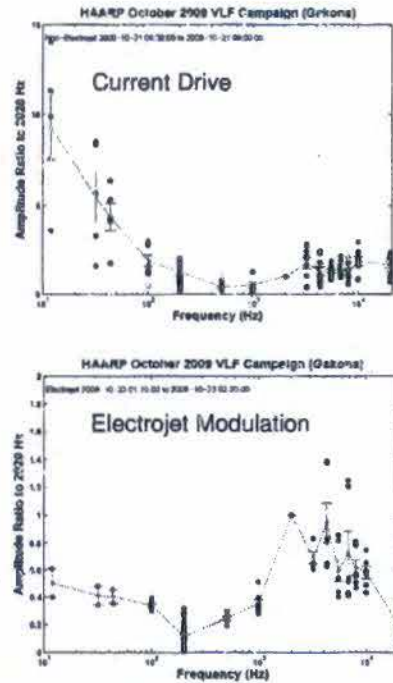


Figure 15 ELF generation efficiency as a function of frequency for top (a) current drive, and bottom (b) electrojet modulation.

4.3. Global ULF Propagation

The ULF campaigns that were conducted under this program are shown in Table 2, from Campaign #3 to #10.

(b)(3):22 USC § 2778(e) Sec 38(e),(b)(4)

(b)(3):22 USC § 2778(e) Sec 38(e),(b)(4)

(b)(3):22 USC § 2778(e) Sec 38(e),(b)(4)

4.3.1. First Evidence of F Layer ICD

(b)(3):22 USC § 2778(e) Sec 38(e),(b)(4)

The first evidence of ULF/ELF generation by modulating the F layer directly in the absence of electrojet current is shown in April 2008 campaign (Campaign #3).

(b)(3)

(b)(3):22 USC § 2778(e) Sec 38(e),(b)(4)

(b)(3):22 USC § 2778(e) Sec 38(e)

The interesting finding is that electrojet at Gakona was non-existent on 4/29.

(b)(3):22 USC § 2778(e) Sec 38(e),(b)(4)

(b)(3):22 USC § 2778(e) Sec 38(e),(b)(4)

(b)(3):22 USC § 2778(e) Sec 38(e),(b)(4)

This is the first tentative evidence in the program to show that ULF waves can be generated by means other than electrojet modulation.

4.3.2. ICD in December 2008 Campaign

The case to generate ULF by direct F layer modulation is much stronger in the December 2008 campaign (Campaign #6). In this campaign, ionospheric modulation at ULF frequencies was performed in evening hours when both D and E layers were absent as shown by the ionosonde at HAARP. Therefore, ULF modulation was directly applied to the F layer and HF power had very low loss going through the lower layers in the ionosphere. Figure 17 shows the ULF vs. 1 kHz amplitudes at Gakona. We can see from this figure that the data points are skewed toward the ULF axis, indicating that ULF amplitudes are much larger than the 1 kHz

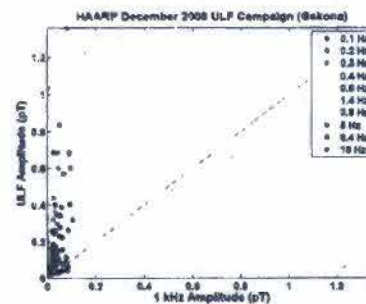


Figure 17. ULF vs. 1 kHz amplitude at Gakona, showing predominant ULF generation at low/no electrojet condition.

amplitudes received on the ground. This suggests that we generated adequate amount of ULF waves through HF modulation, but not by modulating electrojet because otherwise the 1 kHz waves would be strong as well.

(b)(3):22 USC § 2778(e) Sec 38(e),(b)(4)

(b)(3):22 USC § 2778(e) Sec 38(e),(b)(4)

(b)(3):22 USC § 2778(e) Sec 38(e),(b)(4)

4.3.3. (b)(3):22 USC § 2778(e) Sec 38(e),(b)(4) **May 2009 Campaign**

The May 2009 campaign (Campaign #7)

(b)(3):22 USC § 2778(e) Sec 38(e),(b)(4)

(b)(3):22 USC § 2778(e) Sec 38(e),(b)(4) **ULF experiments were performed at evening hours again when there were no lower D/E layers and the F layer was weak, as indicated by low value of foF2 in the local ionosonde.** (b)(3):22 USC § 2778(e) Sec 38(e),(b)(4)

(b)(3):22 USC § 2778(e) Sec 38(e),(b)(4)

(b)(3):22 USC § 2778(e) Sec 38(e),(b)(4)

(b)(3):22 USC § 2778(e) Sec 38(e),(b)(4)

(b)(3):22 USC § 2778(e) Sec 38(e),(b)(4)

(b)(3):22 USC § 2778(e) Sec 38(e),(b)(4)

4.3.4. August 2009 Day Campaign

The August 2009 campaign is different from the earlier ones because it was conducted during the day time, while the earlier campaigns were conducted during the night time when lower D/E layers were absent. In contrast, the ionogram of the August 2009 campaign in Figure 21 shows the presence of D/E layers at altitude from 95 – 180 km range. What make this campaign unique is that we added a temporary observation post at Homer Alaska, which is about 377 miles from Gakona. Because of its proximity to the source, this site also provide near field measurements that were not available in the earlier campaigns.

The observations at Homer came up with 3 ULF events, all at 0.8 Hz, and 35 low ELF events (12-44 Hz) during the campaign. Figure 22 shows the corresponding detection events at Gakona and at Homer. From this figure, we can see that there were many low ELF detections at Homer that were not detected at Gakona. Specifically, on days 08-16, 08-17, and 08-25 the cluster of low ELF events at Homer had no counterpart in Gakona. Moreover, in the period of 08-18 to 08-20, frequent and sometime robust electrojet activities occurred at Gakona. Homer plot shows low number of detections and low amplitude of detected signals in this period. Again, this indicates that there is an anti-correlation between ULF/low ELF distant propagation and electrojet activities at Gakona. Homer plot shows low number of detections and low amplitude of detected signals in this period. Again, this indicates that there is an anti-correlation between ULF/low ELF distant propagation and electrojet activities at Gakona. We speculate that HAARP is located in an ionospheric trough (a highly turbulent region) with strong lateral density gradients that may serve to confine HAARP generated waves from leaving the region. Therefore, it is expected that HF facilities located at mid-lower latitudes, such as Arecibo and Jicamarca, may be more suitable for lateral ULF propagation. We will have to perform ULF generation experiments at these locations in the future to see if there is significant difference in distant detection.

4.3.5. September 2009 Campaign

As the last example of the ULF propagation study, we show the results from the September 2009 campaign (Campaign #9). (b)(3);22 USC § 2778(e) Sec 38(e),(b)(4)

(b)(3);22 USC § 2778(e) Sec 38(e),(b)(4)

(b)(3);22 USC § 2778(e) Sec 38(e),(b)(4)

It is worth noting that the September campaign was focus in the early evening when D/E layers were not present. During the campaign there was no electrojet and ionospheric conditions were quiet at Gakona. (b)(3);22 USC § 2778(e) Sec 38(e),(b)(4)

(b)(3);22 USC § 2778(e) Sec 38(e),(b)(4)

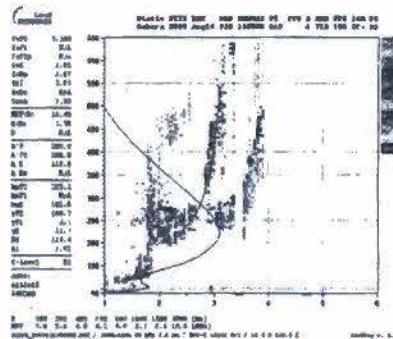
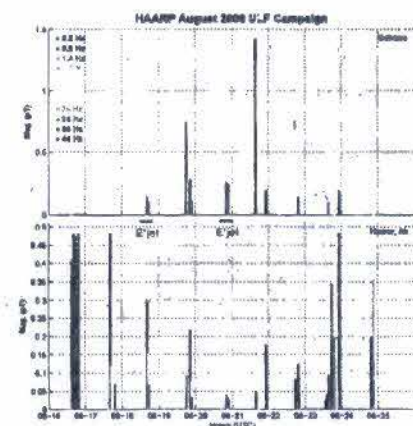


Figure 21. Typical ionogram in August 2009 day campaign.



Day time campaign - Homer site 220 Miles
Figure 22. top (a) amplitude of synchronous ULF diction at Gakona; bottom (b) amplitude of ULF detection at Homer in Campaign #8.

(b)(3):22 USC § 2778(e) Sec 38(e),(b)(4)

(b)(3):22 USC § 2778(e) Sec 38(e),(b)(4)

(b)(3):22 USC § 2778(e) Sec 38(e)

We will connect these observations with the study of ULF propagation models and the results will be presented in the following section.

4.3.6. Summary on ULF Propagation

Based on all the campaign results, we can summary our findings as follows:

- Detection at distant sites does not necessarily means detection at Gakona. There has been significant number of distant events that have no Gakona sighting.

(b)(3):22 USC § 2778(e) Sec 38(e),(b)(4)

4.4. Modeling of ULF Propagation

We have built a simulation model to study global ULF propagation with an excitation source in the ionosphere. The model is based on formulation developed by Lysak [1997] on Alfvénic propagation in 2D geometry that has vertical stratified layers of ionosphere, vertical magnetic field, and homogeneous plasma in the horizontal direction. This model is adequate at high latitude region such as Gakona, AK where magnetic field is predominantly in the vertical direction. However, it does not apply to the mid-low latitude regions because the assumption of vertical magnetic field no longer applies.

We have used this Alfvénic propagation code to simulate horizontal propagation of ULF compressional Alfvén waves produced by a localized source, like the HAARP facility. We have also considered different modes of generation by HF modulation, including

pulsed, continuous, sawtooth sweep, and sinusoidal sweep. In the first year of the program, we conducted parameter survey using this 2D code. In the second year of the program, we upgraded this 2D code to include one more spatial dimension, thus making it a fully 3D code to simulate Alfvénic propagation in three dimensions. From these 2D and 3D simulations, we find that propagation is strongly dependent on F-layer density, with virtually no propagation taking place if F-layer electron number densities are below $10^5/\text{cm}^3$ ($f_oF2 < 3.0$ MHz). Given a robust F-layer ($f_oF2 > 6.0$ MHz), ULF waves can travel to horizontal distances in

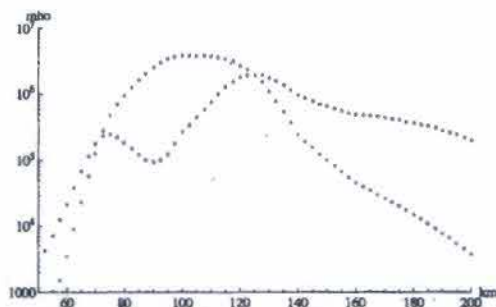


Figure 24. The Hall (red) and Pedersen (blue) conductivities as a function of altitude at the bottom of the ionosphere. The simulation extends down to $z=70$ km. The Hall region, where the Hall conductivity is higher than the Pedersen conductivity, extends from ~ 70 km to ~ 130 km.

excess of 2000 km. However, ground detection of these waves may not be possible because of the so-called "skip distance" effect. This is a common feature in ULF propagation which can be described as follows. After being excited by a source in the F layer, the ULF waves initially travel upwards until they reach the upper boundary of the Alfvénic duct, which is located approximately at an altitude of 4000 km. The ULF waves are then reflected from this boundary in the upper ionosphere and move downward. When the reflected ULF waves reach the lower boundary of the ionosphere, which is the interface between ionosphere and atmosphere, lateral location of the wave front has been shifted by a "skip" distance of the order of 1000 km or so, depending on the frequency of the ULF propagation. Therefore, for a receiver on the ground that is located within the skip distance, no ULF signals will be detected because ULF waves skip pass the receiver position when they reach the bottom of ionosphere.

The simulation region extends from 70 km-8000 km with grid spacing in the vertical (z -) direction that varies from 5 km-250 km in such a way as to always satisfy the Courant condition. In the horizontal (x -) direction it covers 5000 km with a constant horizontal spacing of ~ 40 km. In order to study the effect on propagation of sweeping the heater beam (which breaks the symmetry of the problem) we also developed a 3D version of the code by adding an (y -) direction, which also uses a constant grid spacing of ~ 40 km. The model explicitly advances the compressional and shear Alfvén waves and can use a current drive (see Lysak, 1997), but for our simulations we drove the compressional wave directly at the height where the plasma density is maximum, ~ 370 km. By changing the plasma density we created ionospheric profiles with different F_oF2 frequencies. We kept the conductivity profiles constant throughout our simulations, with a Hall region extending from 70 km-130 km (see Figure 24).

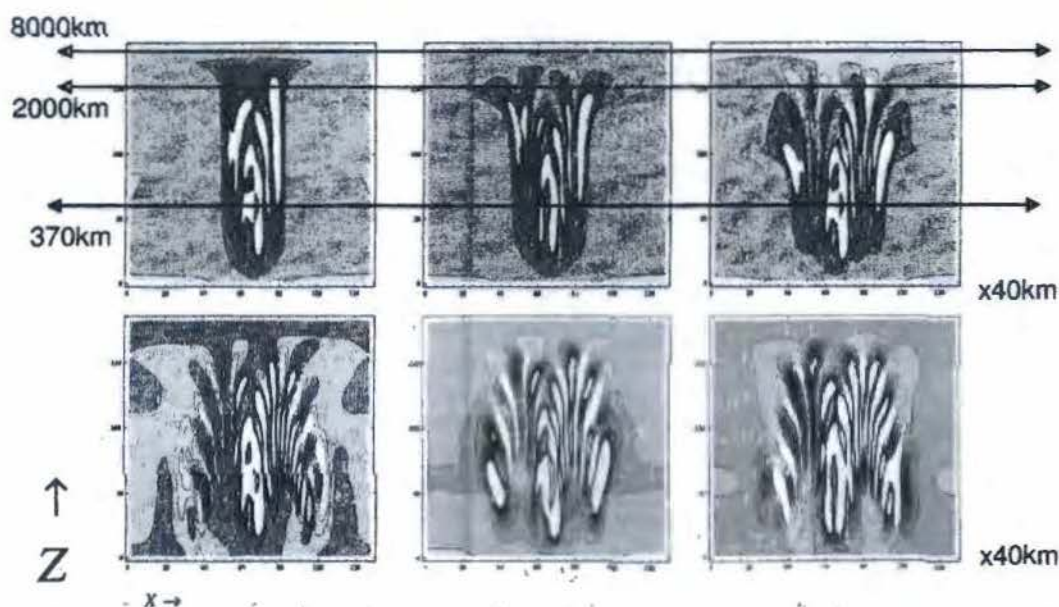


Figure 25. A magnetosonic wave driven at $z = 370$ km by sawtooth sweeping with frequency 1 Hz. We see that the wave propagates first upwards, gets reflected at the upper ionosphere where the plasma density drops, and then propagates down and horizontally along the bottom of the ionosphere. The sawtooth sweep has introduced higher harmonics, and we clearly see the skip distance, a distance of ~ 1000 km where that the magnetosonic waves skip before they reach the bottom of the ionosphere. The horizontal lines show the different heights in the nonuniform z -grid. The minimum of the plasma density is at 3750 km.

Figure 25 shows the propagation of the compressional wave for a sawtooth modulation at 1 Hz. We see that the wave propagates first upwards, gets reflected at the upper ionosphere where the plasma density drops, and then propagates downward and laterally along the bottom of the ionosphere. The sawtooth sweep has introduced higher harmonics, and we clearly see the skip distance, a distance of ~ 1000 km where the magnetosonic waves hop and land at the bottom of the ionosphere. This is a typical picture, exhibited by all cases we have studied.

Figure 26 shows the propagation of the compressional wave at different F layer strength, which is specified by the Alfvénic

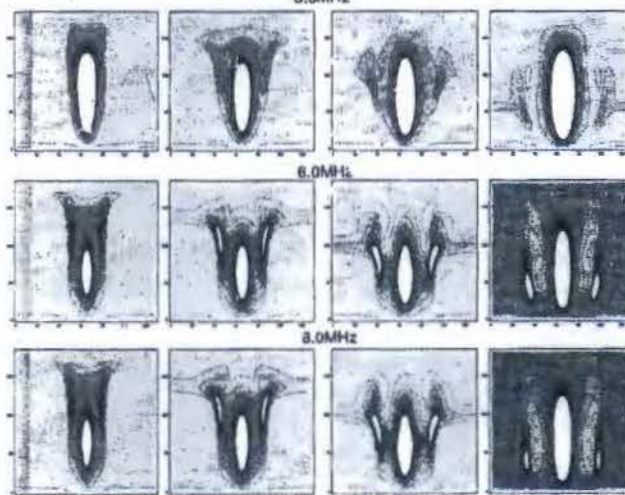
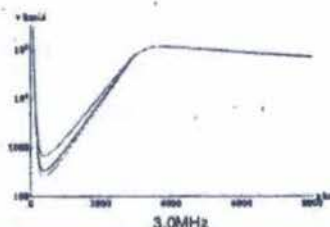


Figure 26. Wave propagation for different foF2 frequencies. The top frame shows the Alfvén speed as a function of height for different foF2 frequencies. A robust F layer ($foF2 > 4$ MHz) is needed for the magnetosonic wave to propagate far along the bottom of the ionosphere.

speed at the F peak. In Figure 26, the top frame shows the model of the Alfvén speed used in each case. We keep the maximum topside Alfvén speed to be $\sim 100,000$ km/s at ~ 3500 km for all three models, and we change the plasma density at ~ 350 km to obtain the corresponding foF2 frequency. In all models the Alfvén speed approaches asymptotically to the speed of light at the ionosphere-atmospheric boundary. In all cases the conductivity profile is the one shown in Figure 24. From Figure 26, we can see that for a weak F-layer (foF2=3MHz) the compressional wave propagates very slowly and barely reaches the bottom of the ionosphere, but for a strong F-layer (foF2=6MHz) it can propagate to long distances along the bottom of the ionosphere.

Based on theory and numerical simulations, we can summarize the major findings from the modeling studies on global ULF propagation characteristics as follows:

Propagation Channels: There are two channels for global ULF propagation. The first channel is the earth-ionospheric waveguide that extends from the ground up to the lower part of the ionosphere. The phenomenon known as Schumann Resonances is the earth cavity modes excited in the earth-ionospheric waveguide. The lowest resonance frequency is at 8 Hz. Below 8 Hz, the ULF propagation is evanescent. Therefore, ULF propagation in this channel has a low cut-off at 8 Hz. The second channel is the Alfvénic duct centers around the F peak. Based on Greifinger's paper [1972] and our simulation, the Alfvénic duct has a low cut-off at 0.2 Hz which is determined by the bounce time between two reflecting boundaries. In addition, there is a high cut-off at 3 Hz. Essentially, dissipation at the lower ionospheric boundary causes strong attenuation for ULF waves above 3 Hz. Therefore, ducted propagation at > 3 Hz can not reach long distances.

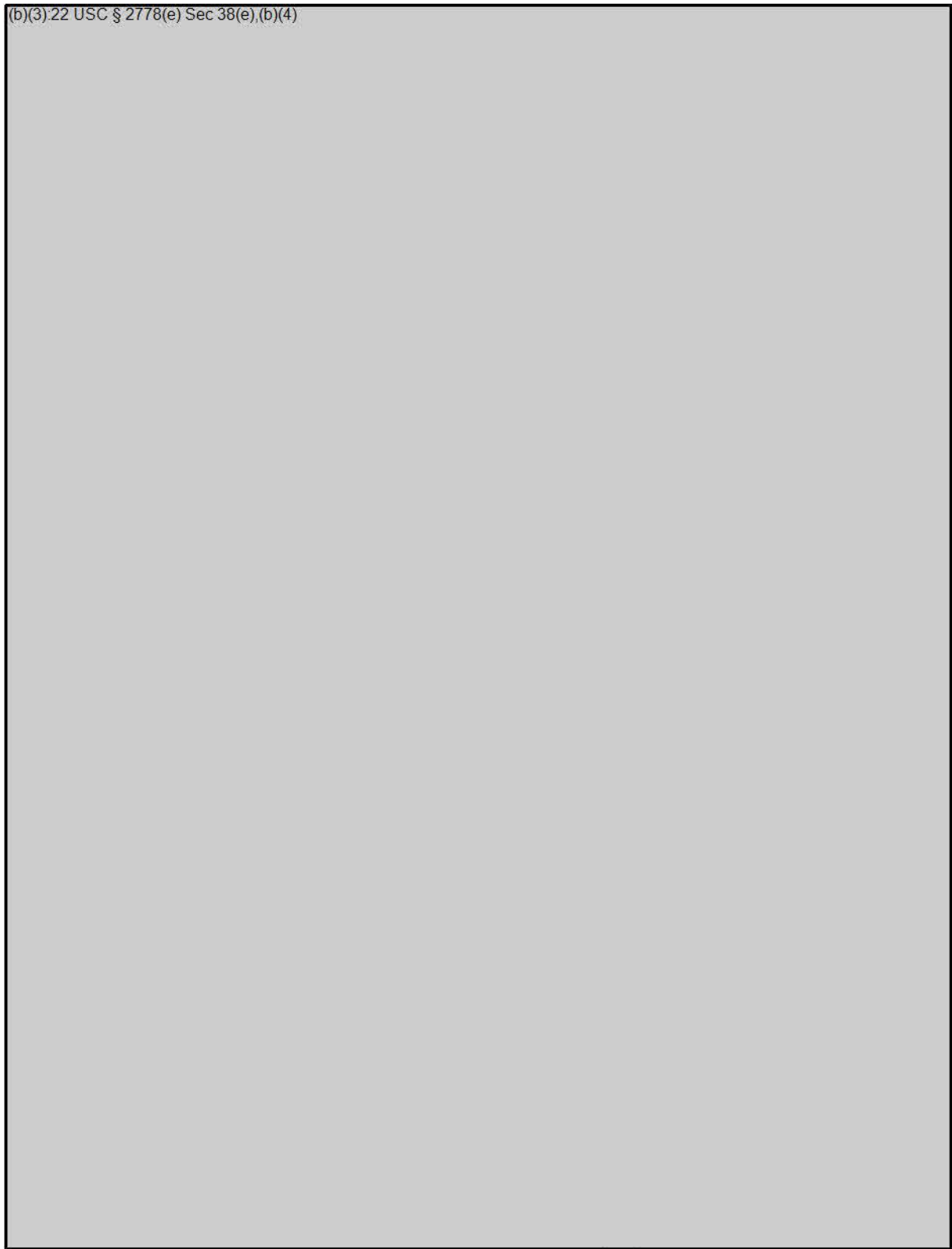
Landing Zone: As mentioned earlier, lateral ULF propagation in the duct are bounced between the duct boundaries, resulting in skip distance as defined by landing zone of the ULF waves reaching the lower boundary of the ionosphere. An important consequence of the skip distance is that ground reception of the lateral propagating ULF waves is only optimized by the receivers located in the landing zone. Therefore, coverage area on the ground will be somewhat restricted by the hopping behavior.

4.5. Satellite Observations

In the first year of the program, satellite observations in sync with HAARP ULF operations were made. The purpose was to measure the effects of ULF modulation and the associated plasma dynamics from space. Several HAARP ULF heating experiments were performed simultaneously with the flyover of the French satellite Demeter. Demeter satellite is designed to detect ionospheric disturbances caused by earthquakes. As such, Demeter satellite carries sophisticated instrument packages to measure E and B waves and plasma properties in its payload. Measurements from these instruments during its flyover HAARP are described below.

4.5.1. ULF signature in space

(b)(3) 22 USC § 2778(e) Sec 38(e),(b)(4)



5. Important Findings and Conclusions

The most important finding in this program is the feasibility of generating ULF and low ELF waves up to 50 Hz by modulating F layer of the ionosphere with HF heater. Since in this approach the heater drives its own current by pressure modulation, it is labeled as ionospheric current drive (ICD). The ICD process is distinctly different from the conventional electrojet modulation because it does not depend on the presence of the electrojet. Therefore, ICD resolves two major problems faced by electrojet modulation: i) the location of the HF facility to be in the electrojet regions; and ii) the highly unpredictable occurrence of the electrojet. Using ICD ULF/ELF waves can be generated by facilities located away from the electrojet regions, as well as in the absence of the electrojet current. The upcoming Arecibo heater in the mid-latitude will be a good candidate to validate the ICD results achieved by HAARP.

Another important result is from data obtained at Homer, AK during August 2009 day campaign (Campaign #8). This campaign is the second ULF campaign conducted in day time and Homer results show that there is an anti-correlation between ULF/low ELF distant propagation and electrojet activities at Gakona. This is a clear indication of non-propagating nature of the ionosphere above HAARP during active electrojet periods. Moreover, the Homer data show many more low ELF events than ULF events in the campaign. This raises interesting questions on the propagation properties of these low ELF waves after being excited by ICD in the F region, and the transferring mechanisms that propagate these waves to the ground. These questions can only be resolved in the future experiments that will require multiple ground receiving station and combined space and ground based low ELF measurements.

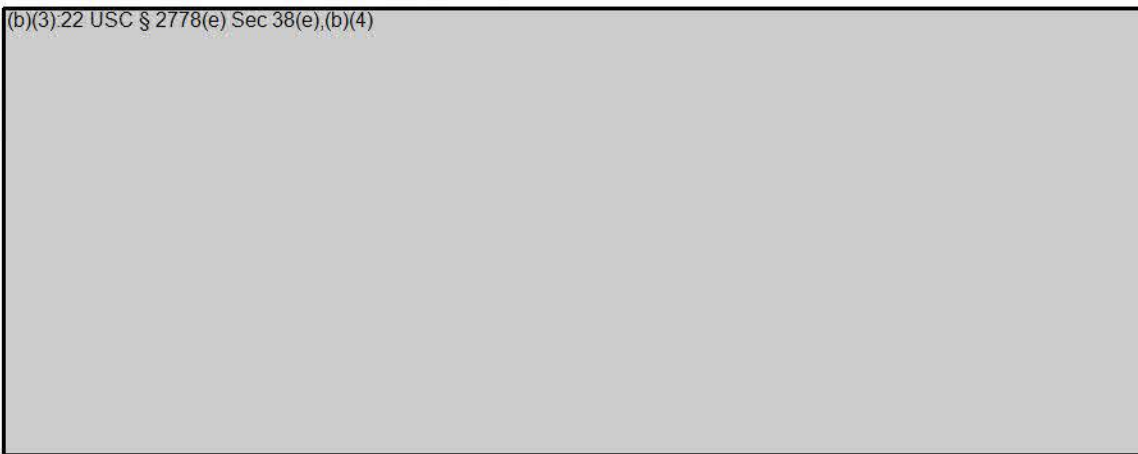
6. Significant Hardware Development

No hardware was developed under this program. All equipment was commercial off the shelf (COTS) products acquired through commercial vendors.

7. Special Comment

No special comment.

(b)(3);22 USC § 2778(e) Sec 38(e),(b)(4)



(b)(3), 22 USC § 2778(e) Sec 38(e), (b)(4)

9. Standard Form 298, September 1988

REPORT DOCUMENTATION PAGE			Form Approved OMB No. 0704-0188	
<p><small>The exact reporting format for this category of information is determined by specific instructions, including the type of reporting organization, reporting activity, reporting period, and reporting requirements. For reporting the report, to the Department of Defense, Standard Form 298 (Rev. 8/73) (GPO: 1974-0-714-114) Reporting should be made to the organization of the report and should be subject to any priority by being in conformity with a contract or otherwise. It does not displace a contract and shall comply with it.</small></p> <p>PLEASE DO NOT RETURN YOUR FORM TO THE ABOVE ORGANIZATION.</p>				
1. REPORT DATE (DD-MM-YYYY) 01-31-2010	2. REPORT TYPE Final Technical Report	3. DATES COVERED (from - to) 1-7-2008-1/7/2010		
4. TITLE AND SUBTITLE Generation & Global Propagation of ULF Waves		5a. CONTRACT NUMBER HR0011-02-C0009	5b. PROGRAM ELEMENT NUMBER	
		5c. GRANT NUMBER	5d. PROJECT NUMBER	
		5e. TAIR NUMBER	5f. WORK UNIT NUMBER	
6. AUTHOR(S) Chia-Lin Chang		7. PERFORMING ORGANIZATION NAME(S) AND ADDRESS(ES) BAE Systems Technology Solutions 2000 N. 15th Street, Suite 1100 Arlington, Virginia 22201		
		8. SPONSORING/MONITORING AGENCY NAME(S) AND ADDRESS(ES) Defense Advanced Research Project Agency Strategic Technology Office (STO) 3701 North Fairfax Drive Arlington, Virginia 22203-1714		
12. DISTRIBUTION/AVAILABILITY STATEMENT		10. SPONSORING/MONITORING AGENCY REPORT NUMBER ARPA Order No. X13600, Prog Code 7F		
13. SUPPLEMENTARY NOTES				
14. ABSTRACT The High Frequency Active Auroral Research Program (HAARP) has the world's most advanced ionospheric research facility. The first goal of this project is to develop the technology of generating Ultra Low Frequency (ULF) waves in the 0.1-10 Hz frequency range using HAARP. The second goal of this project is to explore the propagation characteristics of these artificial ULF waves to global locations. Results from HAARP campaigns show that ULF and ELF waves from 0.1 to 50 Hz can be generated consistently without relying on the presence of electrojet. The non-electrojet generation mechanism is driving plasma currents in F layer of the ionosphere by powerful HF modulation from HAARP. This mechanism is also known as ionospheric current drive (ICD), to distinguish it from the conventional electrojet modulation method in the D/E regions.				
15. SUBJECT TERMS				
16. SECURITY CLASSIFICATION OF:		17. LIMITATION OF ABSTRACT	18. NUMBER OF PAGES	19a. NAME OF RESPONSIBLE PERSON
2. REPORT	5. ABSTRACT	8. THIS PAGE	119.	19b. TELEPHONE NUMBER (include area code)
				David

10. References

Greifinger, Carl, and Phillis Greifinger, "Approximate Method for Determining ELF Eigenvalues in the Earth-Ionosphere Waveguide", *Radio Science*, Vol. 13, No. 5, p.831-837, 1978.

Greifinger, Carl, and Phillis Greifinger, "On the Ionospheric Parameters Which Govern High-Latitude ELF Propagation in the Earth-Ionosphere Waveguide", *Radio Science*, Vol. 14, No. 5, p.889-895, 1979.

Lysak, R. L., "Propagation of Alfvén Waves Through the Ionosphere", *Phys. Chem. Earth*, 22, 757, 1997.

Parrot, M, J. J. Berthelier, J. P. Lebreton, *et al.*, "Examples of Unusual Ionospheric Observations Made by the DEMETER Satellite Over Seismic Regions", *Physics and Chemistry of the Earth*, Vol. 31, p. 486-495, 2006.